Etch-Induced Ion Exchange Engineering of Two-Dimensional Layered NiFeCo-Based Hydroxides for High-Energy Charge Storage

a. Chenhan Xiong [a,#], Wei Cao [a,#], Qiang Long [a], Jiaqi Chen [a], Yanqiu Yu [a], Xinming Lian [a], Jianhua Huang [b,c], Guoping Du [a], Nan Chen [a,*]

b. School of Materials Science and Engineering, Nanchang University, Nanchang 330031, China

# These authors (C. Xiong and W.Cao) contributed equally to this article.

* Corresponding authors, emails: nanchen@ncu.edu.cn (NC)

Figure Captions and Video

Fig. S1 Photographic images of the beginning and ending of the electrochemical synthesis process, and of pure NF, NF after etching treatment, and NF after electrochemical synthesis.

Fig. S2 Photographic images of pre-treatment pure NF (a), Ni/NF (b), $Ni_1Fe_{0.1}$/NF (c), $Ni_1Fe_{0.3}$/NF (cd) and $Ni_1Fe_{0.5}$/NF (e).

Fig. S3 SEM images of pure NF (a, b), Ni/NF (c, d), $Ni_1Fe_{0.1}$/NF (e, f), $Ni_1Fe_{0.3}$/NF (g, h) and $Ni_1Fe_{0.5}$/NF (g, h).

Fig. S4 SEM image (a) and XRD pattern (b) of the pretreated NF.

Fig. S5 XRD patterns of the series of electrochemical in situ grown electrodes.

Fig. S6 (a) CV and (b) GCD curves of the series of electrodes at a scan rate of 10 mV s^{-1} and a current density of 2 mA cm^{-2}, respectively. (c) CV curves of $Ni_1Fe_{0.5}$/NF electrode with scan rates from 2 to 50 mV s^{-1}, (d) GCD curves of $Ni_1Fe_{0.5}$/NF electrode with current densities from 2 to 10 mA cm^{-2}. (e) Specific capacity of the series of electrodes at various current densities.

Fig. S7 Series of electrode CV and GCD curves with scan rates from 2 to 50 mV s^{-1} and current density from 2 to 10 mA cm^{-2}, (a, e) Ni/NF, (b, f) $Ni_1Fe_{0.1}$/NF, (c, g) $Ni_1Fe_{0.3}$/NF and (d, h) $Ni_1Fe_{0.5}$/NF.

Fig. S8 Series of electrode CV and GCD curves with scan rates from 2 to 50 mV s^{-1} and current density from 2 to 10 mA cm^{-2}, (a, d) $Ni_1(Fe/Co=2/1)_{0.5}$/NF, (b, e) $Ni_1(Fe/Co=1/2)_{0.5}$/NF and (c, f) $Ni_1Co_{0.5}$/NF.

Fig. S9 (a) Photographic images of the beginning and ending of the electrochemical synthesis process for unpretreated NF, (b) SEM image, (c) XRD pattern, (d) CV and (e) GCD curves.

Fig. S10 XPS of the pretreated NiFeCo/NF.

Fig. S11 Cycling performances of the series of electrodes.

Fig. S12 SEM images of (a) before cycling test, and (b) after cycling test, with (c) TEM image and (d) SAED pattern of after cycling test.

Fig. S13 Negative electrode (a) CV curves with the scan rates from 2 to 100 mV s^{-1}, and (b) GCD curves with the current density from 1 to 10 mA cm^{-2}.

Fig. S14 CV curves of $Ni_1(Fe/Co=1/1)_{0.5}$/NF and AC electrodes at the scan rate of 10 mV s^{-1}.

Fig. S15 Photographic image of $Ni_1(Fe/Co=1/1)_{0.5}$/NF //AC HSC device driving LED lamp combination.

Video. S1 A typical video recording process of in situ electrochemical synthesis of transition metal-based hydroxides on NF ($Ni_1(Fe/Co=1/1)_{0.5}$/NF).

Table. S1 Comparison of electrochemical performance of related literature on transition metal-based hydroxides electrodes.

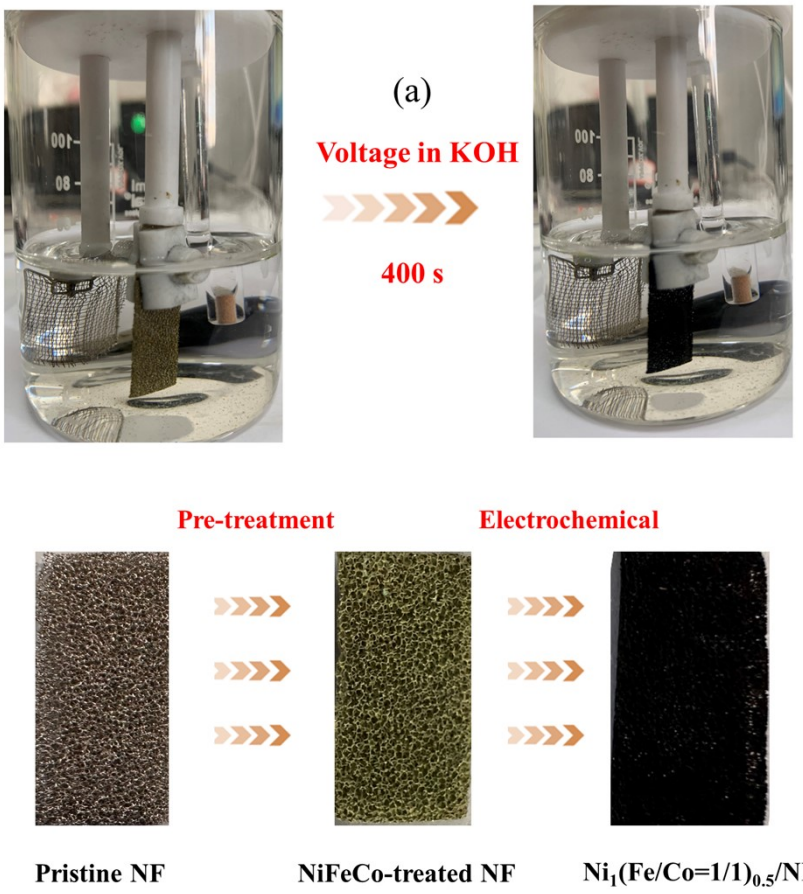

Fig. S1 Photographic images of the beginning and ending of the electrochemical synthesis process, and of pure NF, NF after etching treatment, and NF after electrochemical synthesis.

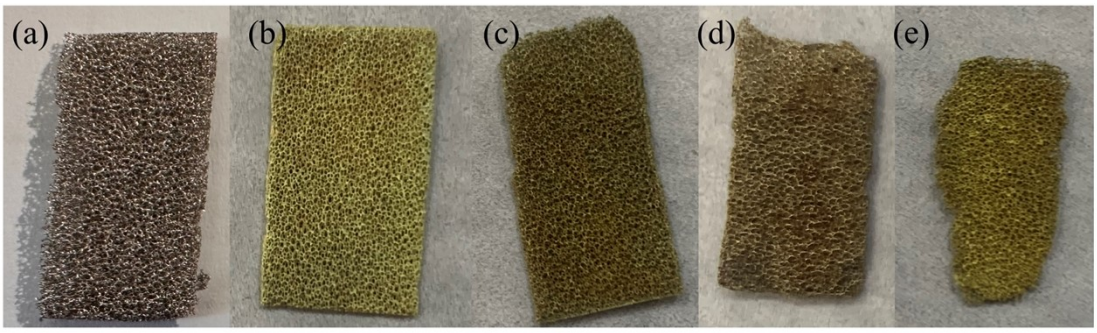

Fig. S2 Photographic images of pre-treatment pure NF (a), Ni/NF (b), $Ni_1Fe_{0.1}$/NF (c), $Ni_1Fe_{0.3}$/NF (cd) and $Ni_1Fe_{0.5}$/NF (e).

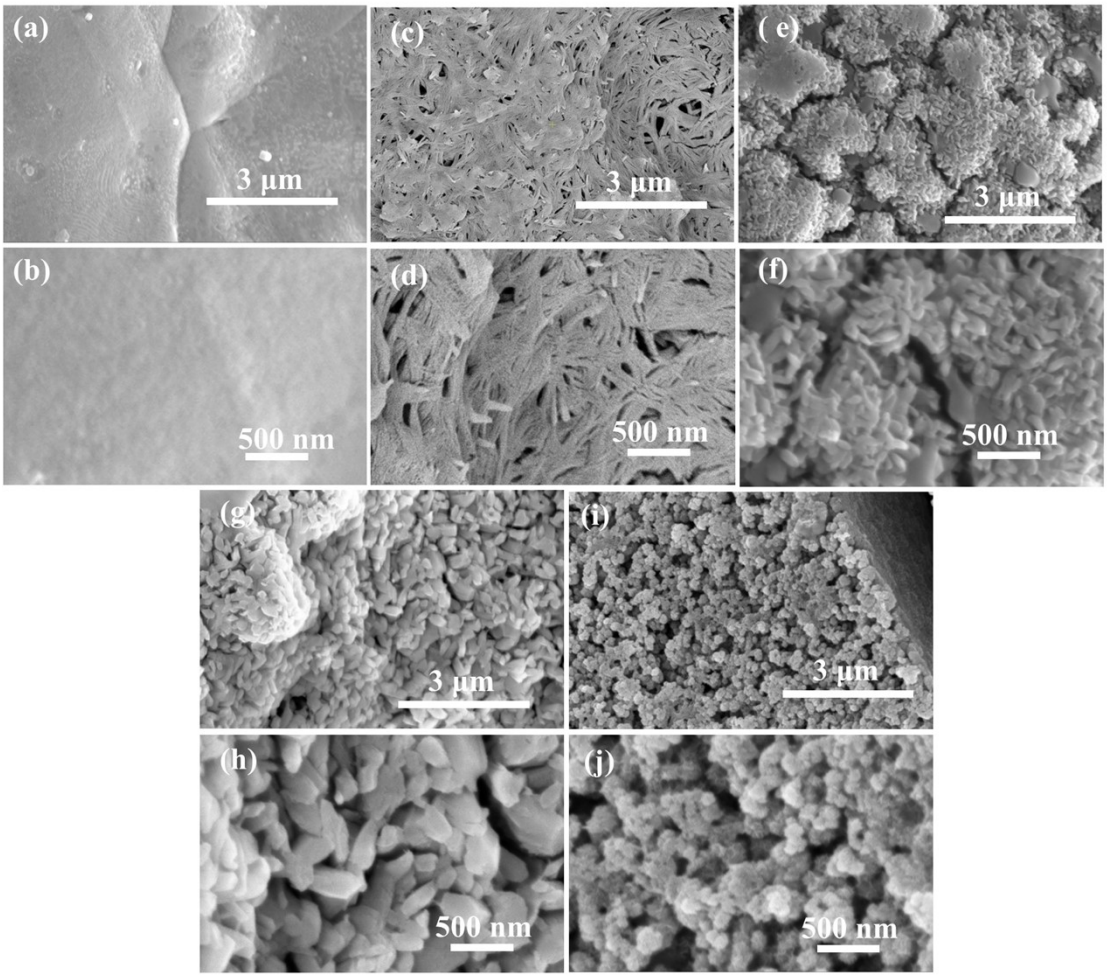

Fig. S3 SEM images of pure NF (a, b), Ni/NF (c, d), $Ni_1Fe_{0.1}$/NF (e, f), $Ni_1Fe_{0.3}$/NF (g, h) and $Ni_1Fe_{0.5}$/NF (g, h).

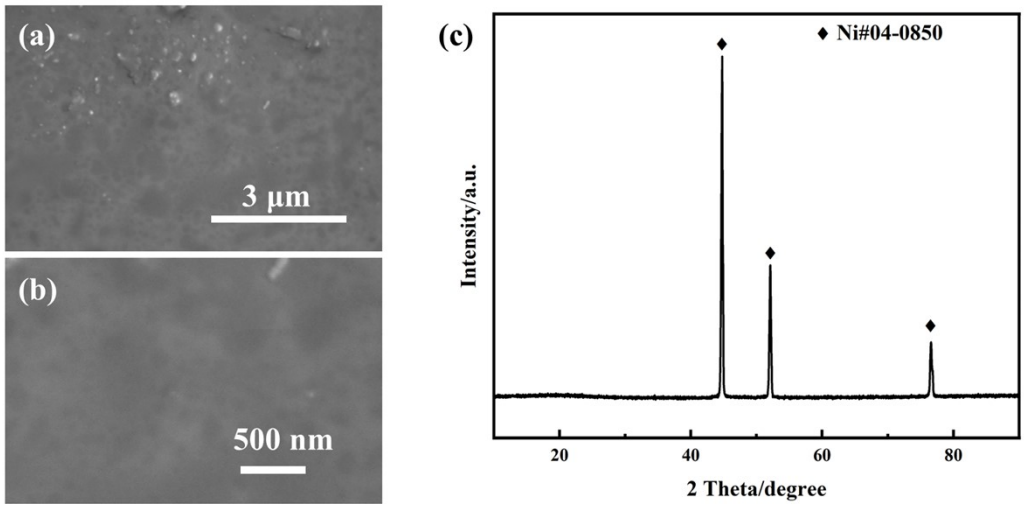

Fig. S4 SEM image (a) and XRD pattern (b) of the pretreated NF.

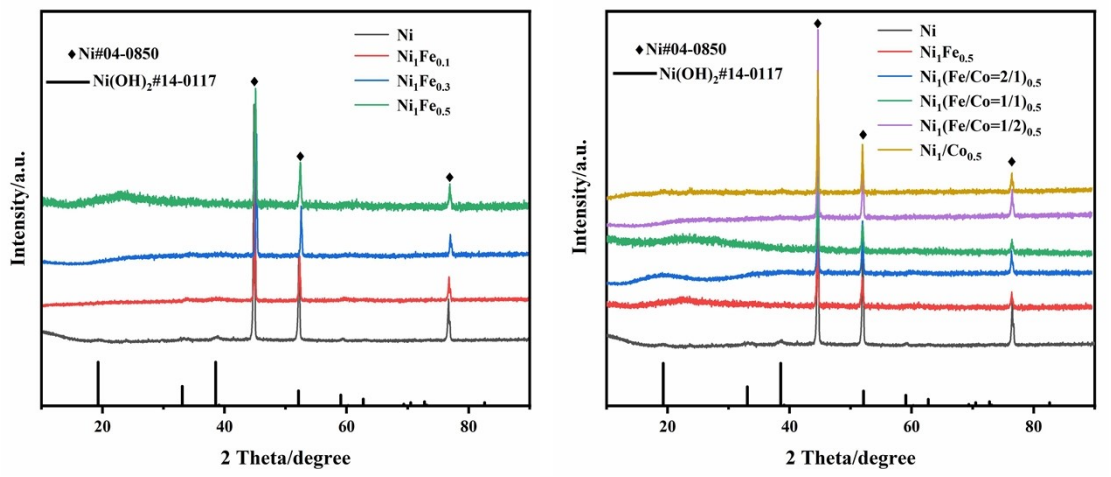

Fig. S5 XRD patterns of the series of electrochemical in situ grown electrodes.

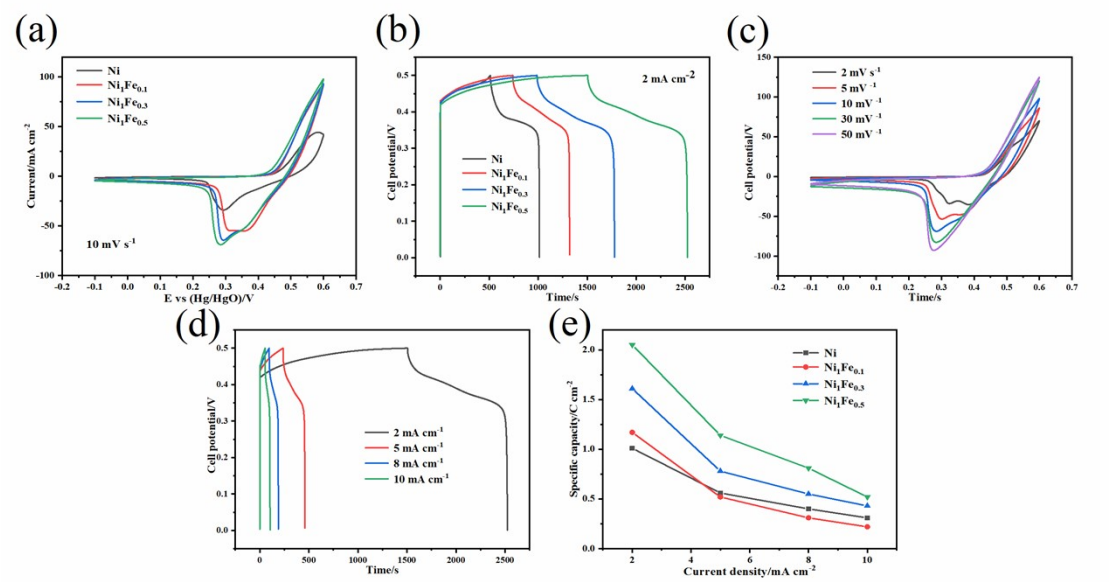

Fig. S6 (a) CV and (b) GCD curves of the series of electrodes at a scan rate of 10 mV s^{-1} and a current density of 2 mA cm^{-2}, respectively. (c) CV curves of $Ni_1Fe_{0.5}$/NF electrode with scan rates from 2 to 50 mV s^{-1}, (b) GCD curves of $Ni_1Fe_{0.5}$/NF electrode with current densities from 2 to 10 mA cm^{-2}. (e) Specific capacity of the series of electrodes at various current densities.

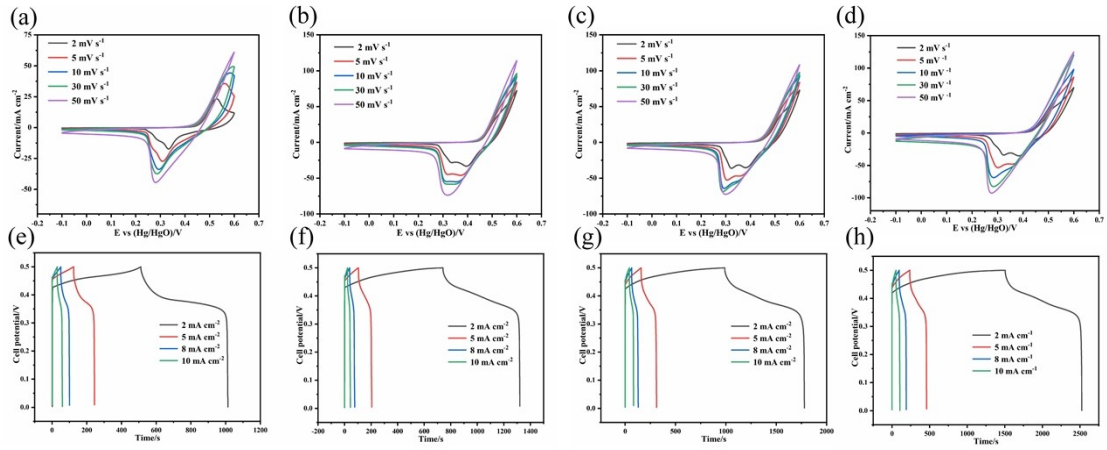

Fig. S7 Series of electrode CV and GCD curves with scan rates from 2 to 50 mV s^{-1} and current density from 2 to 10 mA cm^{-2}, (a, e) Ni/NF, (b, f) $Ni_1Fe_{0.1}$/NF, (c, g) $Ni_1Fe_{0.3}$/NF and (d, h) $Ni_1Fe_{0.5}$/NF.

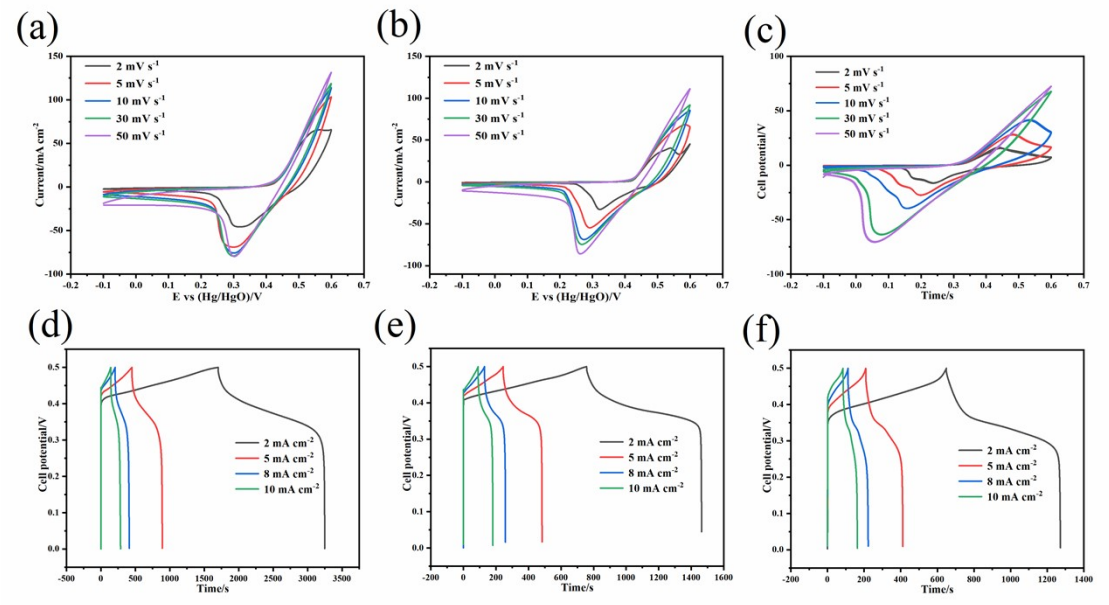

Fig. S8 Series of electrode CV and GCD curves with scan rates from 2 to 50 mV s^{-1} and current density from 2 to 10 mA cm^{-2}, (a, d) $Ni_1(Fe/Co=2/1)_{0.5}$/NF, (b, e) $Ni_1(Fe/Co=1/2)_{0.5}$/NF and (c, f) $Ni_1Co_{0.5}$/NF.

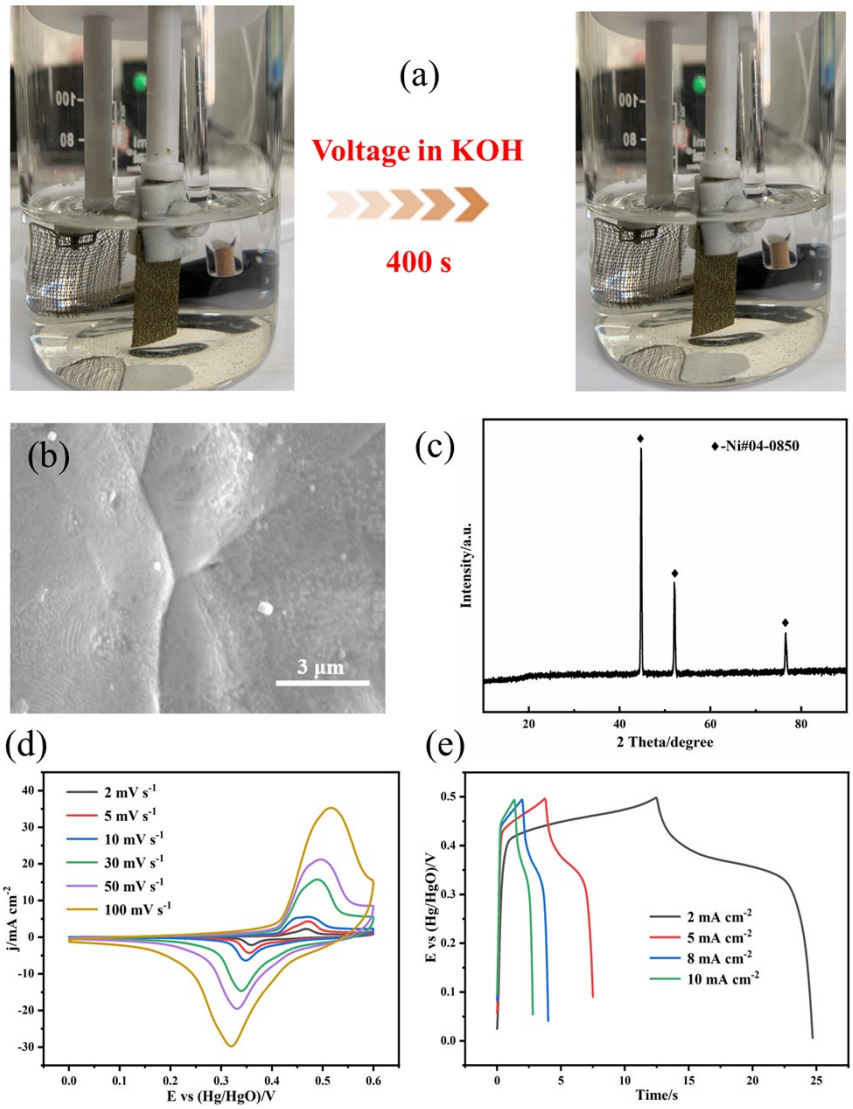

Fig. S9 (a) Photographic images of the beginning and ending of the electrochemical synthesis process for unpretreated NF, (b) SEM image, (c) XRD pattern, (d) CV and (e) GCD curves.

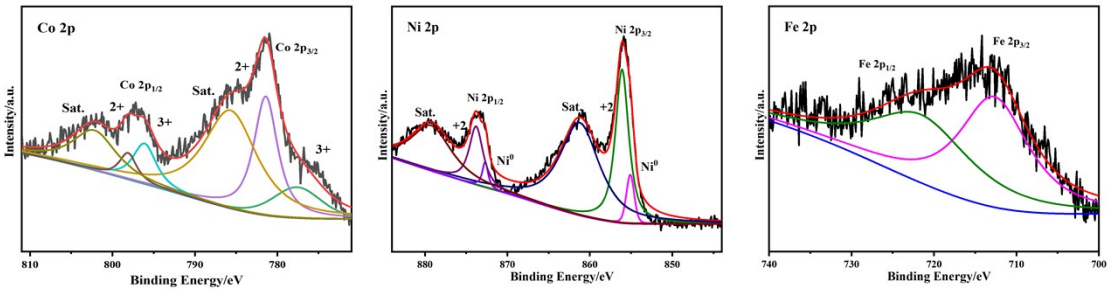

Fig. S10 XPS of the pretreated NiFeCo/NF.

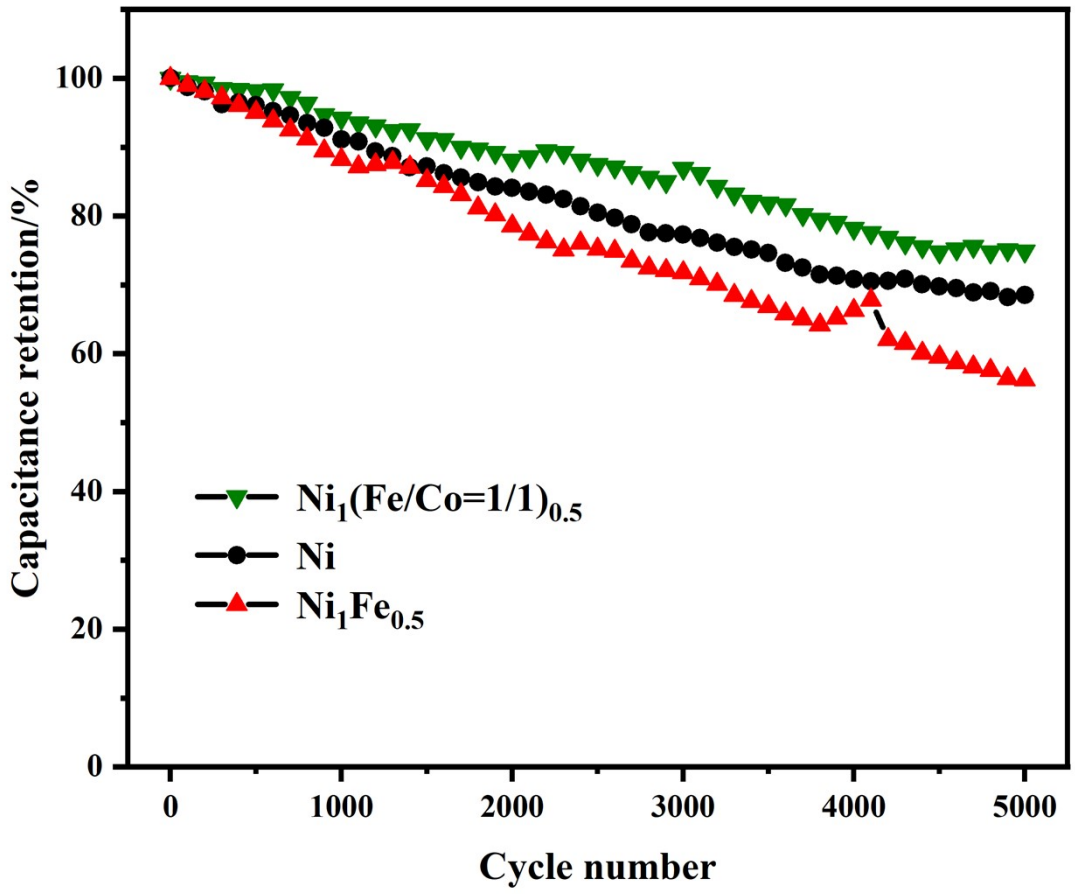

Fig. S11 Cycling performances of the series of electrodes.

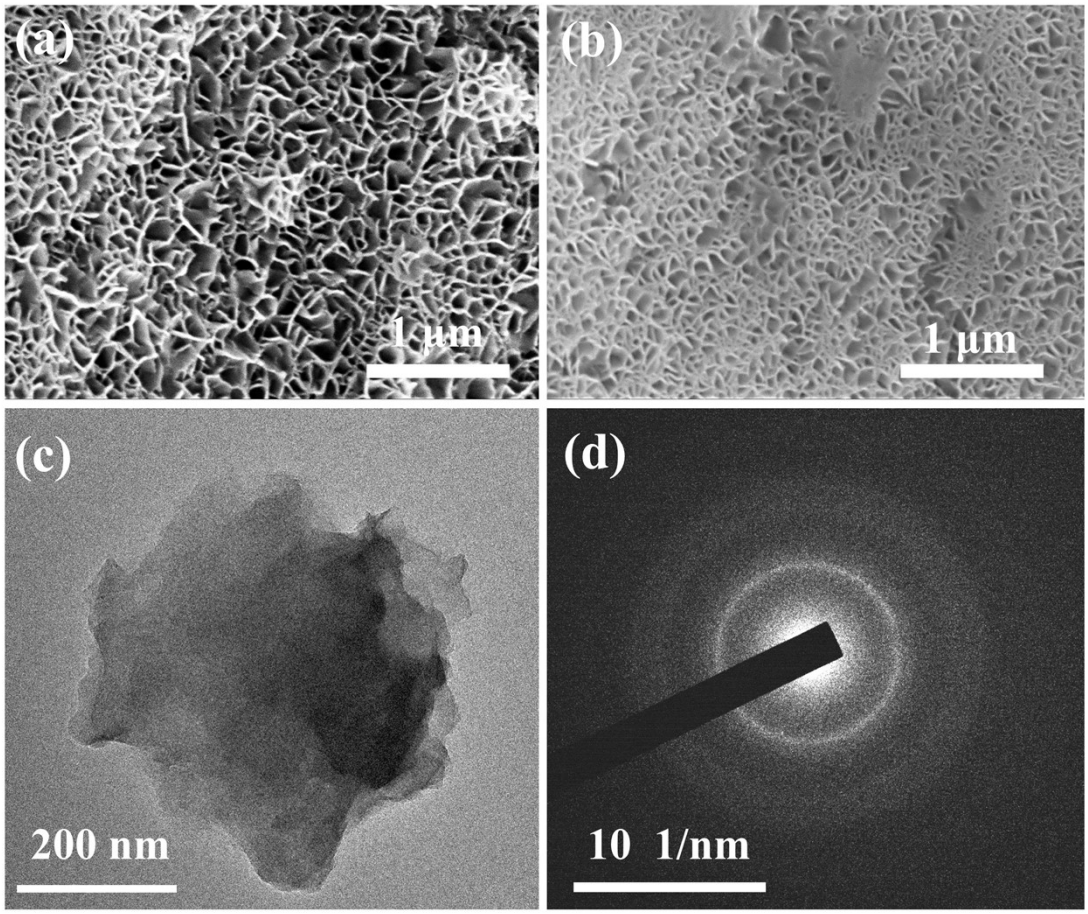

Fig. S12 SEM images of (a) before cycling test, and (b) after cycling test, with (c) TEM image and (d) SAED pattern of after cycling test.

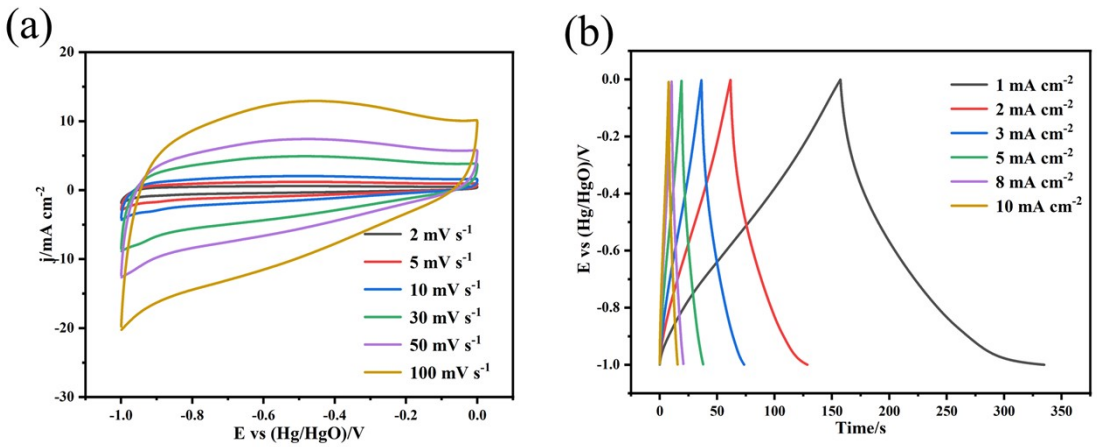

Fig. S13 Negative electrode (a) CV curves with the scan rates from 2 to 100 mV s^{-1}, and (b) GCD curves with the current density from 1 to 10 mA cm^{-2}.

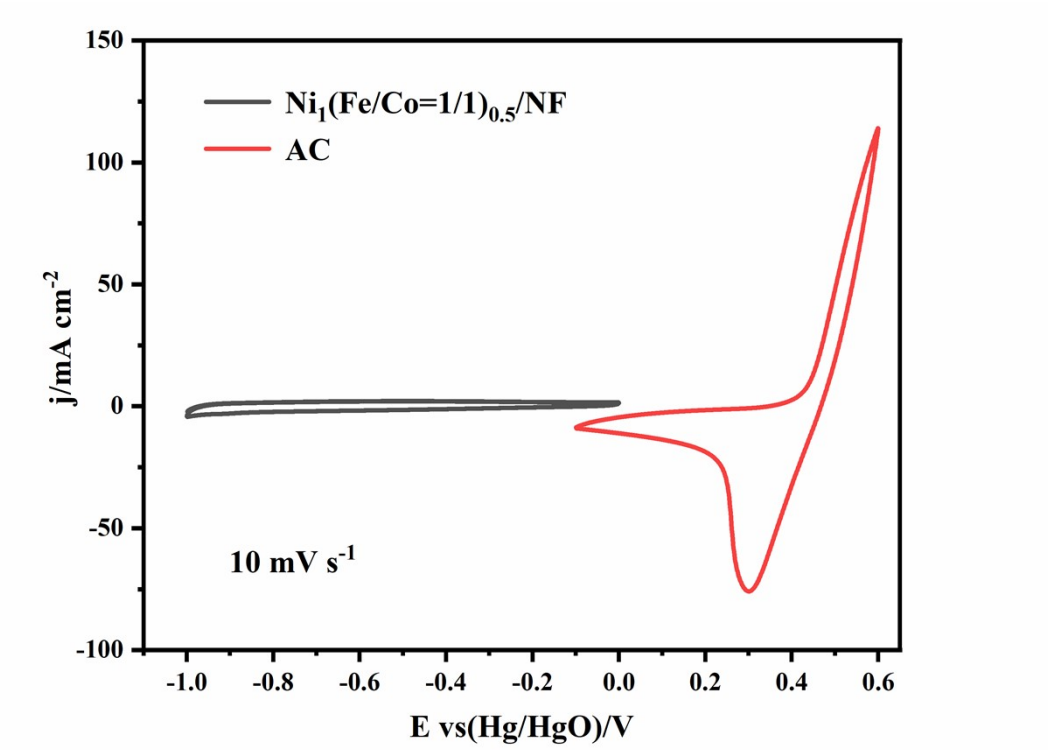

Fig. S14 CV curves of $Ni_1(Fe/Co=1/1)_{0.5}$/NF and AC electrodes at the scan rate of 10 mV s^{-1}.

Fig. S15 Photographic image of $Ni_1(Fe/Co=1/1)_{0.5}$/NF //AC HSC device driving LED lamp combination.

a75be05c6dc9f7
50065fa2249fdb(

Video. S1 A typical video recording process of in situ electrochemical synthesis of transition metal-based hydroxides on NF ($Ni_1(Fe/Co=1/1)_{0.5}$/NF).

Table. S1 Comparison of electrochemical performance of related literature on transition metal-based hydroxides electrodes.

Electrode materials	Technical route/synthesis time	Specific capacitance	Current density	Ref.
NC LDH NSs@Ag@CC	Two-step method/High temperature for a long time	1111.7 F cm^{-2} (502.9 mC cm^{-2})	2 mA cm^{-2}	[1]
Co_9S_8/PPy/NiCo-LDH NTAs	Three-step method/19 h	2.65 F cm^{-2} (1325 mC cm^{-2})	1 mA cm^{-2}	[2]
NiCo-LDH/Mn_3O_4	Two-step method/25 min	1.86 C cm^{-2}	1 mA cm^{-2}	[3]
H-NiCo LDH/ACC	Two-step method/25 h	1377 mC cm^{-2}	1 mA cm^{-2}	[4]
NiO@MnO_2	Two-step method/26 h	119.4 F cm^{-2} (83.6 mC cm^{-2})	2 mA cm^{-2}	[5]
Co-Ni LDH–CC–CNT	Three--step method/3 h	1979.2 F cm^{-2} (1187.5 mC cm^{-2})	1 mA cm^{-2}	[6]
$Ni(OH)_2$ NTAs	Two-step method/5 h	315 F cm^{-2} (157.5 mC cm^{-2})	18 mA cm^{-2}	[7]
$Ni_1(Fe/Co=1/1)_{0.5}$/NF	One-step method/400 s	2.32 C cm^{-2}	2 mA cm^{-2}	This work

Note: The purpose of the technical route/synthesis time listed in Table. S1 is to reflect efficiency of the strategy proposed in this work. In particular, the technical route refers to the steps required for the synthesis of materials reported in the literature, and the synthesis time refers to the sum of time spent in the synthesis stage of materials.

References

[1] S. C. Sekhar, G. Nagaraju, and J. S. Yu, "Conductive silver nanowires-fenced carbon cloth fibers-supported layered double hydroxide nanosheets as a flexible and binder-free electrode for high-performance asymmetric supercapacitors," *Nano Energy,* vol. 36, pp. 58-67, 2017.

[2] L. Wang, S. Li, F. Huang, X. Yu, M. Liu, and H. Zhang, "Interface modification of hierarchical Co_9S_8@NiCo layered dihydroxide nanotube arrays using polypyrrole as charge transfer layer in flexible all-solid asymmetric supercapacitors," *Journal of Power Sources,* vol. 439, 2019.

[3] N. Zhao *et al.*, "Preparation of partially-cladding NiCo-LDH/Mn_3O_4 composite by electrodeposition route and its excellent supercapacitor performance," *Journal of Alloys and Compounds,* vol. 796, pp. 111-119, 2019.

[4] X. Xuan *et al.*, "In-situ growth of hollow NiCo layered double hydroxide on carbon substrate for flexible supercapacitor," *Electrochimica Acta,* vol. 321, 2019.

[5] X. Liu, J. Wang, and G. Yang, "Amorphous nickel oxide and crystalline manganese oxide nanocomposite electrode for transparent and flexible supercapacitor," *Chemical Engineering Journal,* vol. 347, pp. 101-110, 2018.

[6] C. Xu, X. Kong, S. Zhou, B. Zheng, F. Huo, and M. Strømme, "Interweaving metal–organic framework-templated Co–Ni layered double hydroxide nanocages with nanocellulose and carbon nanotubes to make flexible and foldable electrodes for energy storage devices," *Journal of Materials Chemistry A,* vol. 6, no. 47, pp. 24050-24057, 2018.

[7] C. Shi, J. Sun, Y. Pang, Y. Liu, B. Huang, and B. T. Liu, "A new potassium dual-ion hybrid supercapacitor based on battery-type $Ni(OH)_2$ nanotube arrays and pseudocapacitor-type V_2O_5-anchored carbon nanotubes electrodes," *J Colloid Interface Sci,* vol. 607, no. Pt 1, pp. 462-469, Feb 2022.